PCCP

Accepted Manuscript

ROYAL SOCIETY OF CHEMISTRY

rsc.li/pccp

View Article Online
DOI: 10.1039/C8CP00382C

Journal Name

ARTICLE

Received 00th January 20xx,

Accepted 00th January 20xx

DOI: 10.1039/x0xx00000x

www.rsc.org/

Supramolecular Complex of a Fused Zinc Phthalocyanine-Zinc Porphyrin Dyad Assembled by Two Imidazole-C_{60} Units: Ultrafast Energy Transfer Followed by Electron Transfer

Jorge Follana-Berná,[a] Sairaman Seetharaman,[b] Luis Martín-Gomis,[a] Georgios Charalambidis,[d] Adelais Trapali,[d] Paul A. Karr,[c] Athanassios G. Coutsolelos,[d] Fernando Fernández-Lázaro,[a] Francis D'Souza*[b] and Ángela Sastre-Santos*[a]

A new zinc phthalocyanine-zinc porphyrin dyad (ZnPc-ZnP) fused through a pyrazine ring has been synthesized as a receptor for imidazole-substituted C_{60} (C_{60}Im) electron acceptor. Self-assembly via metal-ligand axial coordination and the pertinent association constants in solution were determined by ^{1}H-NMR, UV-Vis and fluorescence titration experiments at room temperature. The designed host was able to bind up to two C_{60}Im electron acceptor guest molecules to yield C_{60}Im:ZnPc-ZnP:ImC_{60} donor-acceptor supramolecular complex. The spectral data showed that the two binding sites behave independently with binding constants similar in magnitude. Steady-state fluorescence studies were indicative of an efficient singlet-singlet energy transfer from zinc porphyrin to zinc phthalocyanine within the fused dyad. Accordingly, the transient absorption studies covering a wide timescale of femto-to-milli seconds revealed ultrafast energy transfer from ^{1}ZnP* to ZnPc (k_{EnT} ~ 10^{12} s^{-1}) in the fused dyad. Further, a photo induced electron transfer was observed in the supramolecularly assembled C_{60}Im:ZnPc-ZnP:ImC_{60} donor-acceptor complex leading to charge separated states, which persisted for about 200ns.

Introduction

There is an increasing interest in the design and synthesis of novel conjugated two-dimensional covalent molecular systems for their application in the areas of optoelectronic,[1–7] optical data storage[6] and light energy harvesting.[8–15] Phthalocyanines (Pc)[16–20] and porphyrins (P)[21,22] have emerged as building blocks for the construction of new materials due to their thermal, chemical and photochemical stability. Moreover, the complementary absorptions of both units have increased the interest in covalently fused Pc-P dyads as they cover a wider range of the solar spectrum, and consequently have generated a great expectation for photovoltaic applications.[23–29] Various Pc-P covalently connected systems with different linkers have been synthesized, which could be utilized as possible light harvesting architectures.[30] The good overlap between the emission of porphyrin with the Q band absorption of phthalocyanine in most Pc-P conjugates gives rise to an efficient intramolecular energy transfer from singlet excited porphyrin to phthalocyanine core.[13,14,23–29,31–38] Further, appending one or two electron acceptor entities to the Pc-P dyads make such supramolecular donor-acceptor systems photochemically more attractive as they reveal charge separation upon photoexcitation.[13,14,31,32]

A literature survey on the Pc-P-C_{60} triads reveal several interesting features of the supramolecular construction. Conjugated Pc-P dyads in which the phthalocyanines are directly linked to the β-pyrrolic position of a *meso*-tetra-phenylporphyrin have been prepared and their photophysical processes have been studied by assembling pyridylfulleropyrrolidine through metal-ligand coordination.[33] In a parallel study, using a *two-point* binding strategy, a Pc-C_{60}-P triad was assembled and occurrence of sequential energy and electron transfer events was demonstrated.[34] Synthesis and photochemistry of several Pc–C_{60}–P triads covalently connected by a pyrrolidine spacer have also been reported.[35] Recently, a non-fused ZnPc-ZnP system supramolecularly connected with two C_{60} units has been described by us.[36] Detailed photochemical studies of this triad revealed charge stabilization via an electron/hole transfer mechanism. Finally, supramolecular hybrid systems based on distorted fused ZnP–ZnPc conjugates and a pyridylfullerene have also been described,[37] and their photophysical measurements

[a] *División de Química Orgánica, Instituto de Bioingeniería Universidad Miguel Hernández Avda. de la Universidad s/n 03203 Elche, Spain E-mail: asastre@umh.es*
[b] *Department of Chemistry University of North Texas at Denton 1155 Union Circle, #305070, Denton, TX 76203-5017, USA E-mail: francis.dsouza@unt.edu*
[c] *Department of Physical Sciences and Mathematics, Wayne State College, 111 Main Street, Wayne, Nebraska 68787, USA*
[d] *Departement of Chemistry, University of Crete, Laboratory of Bioinorganic Chemistry, Voutes Campus, 70013 Heraklion, Crete, Greece*
†Electronic Supplementary Information (ESI) available: See DOI: 10.1039/x0xx00000x

View Article Online
DOI: 10.1039/C8CP00382C

corroborate a sequential deactivation in the excited state, namely an initial intramolecular energy transfer from ZnP to ZnPc followed by an intramolecular charge transfer to yield ZnP–(ZnPc)$\cdot^{+}$–(C_{60})$\cdot^{-}$ charge separated state.

Supramolecular interaction of planar fused porphyrin dimers and C_{60} was recently described by Aida and coworkers where a single unit of C_{60} was complexed, while the introduction of a second fullerene moiety was hindered by a strong negative cooperative effect. In this case, the electronic communication between the two fused porphyrins caused a decrease of the affinity of the receptor toward the second C_{60} unit.[38] Moreover, Martín, Nierengarten and coworkers reported two conjugated porphyrin-based systems endowed with suitable crown ether receptors for a fullerene-ammonium salt derivative presenting negative cooperativity in both cases, although in one of the systems the negative effect was weaker due to fullerene-fullerene interactions in the 2:1 supramolecular assembly.[39] In this context, it would be interesting to investigate the complexation properties of a planar fused ZnPc-ZnP system with a fullerene-imidazole ligand to generate a photoactive supramolecular system.

Studies on Pc-P dyads performed to-date have revealed that most of these dyads are not planar with respect to the relative macrocycle geometry and orientation. It is known that excitation transfer is facilitated in energy harvesting donor-acceptor dyads possessing planar geometry that would also facilitate binding of electron acceptors through metal-ligand axial coordination with minimal steric crowding.[32] In the present study, we have synthesized a new ditopic conjugated zinc phthalocyanine-zinc porphyrin dyad linked through a pyrazine ring (ZnPc-ZnP, Scheme 1), to verify these predictions. Due to direct ring fusion, the two rings are arranged in the same plane. Further, the Zn centers were coordinated with imidazole substituted C_{60} to form donor-acceptor supramolecular complex (C_{60}-Im:ZnPc-ZnP:Im-C_{60}, Scheme 2). The formation of the supramolecular system and photochemical events originating upon excitation have been systematically investigated using various spectral, computational, electrochemical and photochemical techniques, and are summarized in the following sections.
.

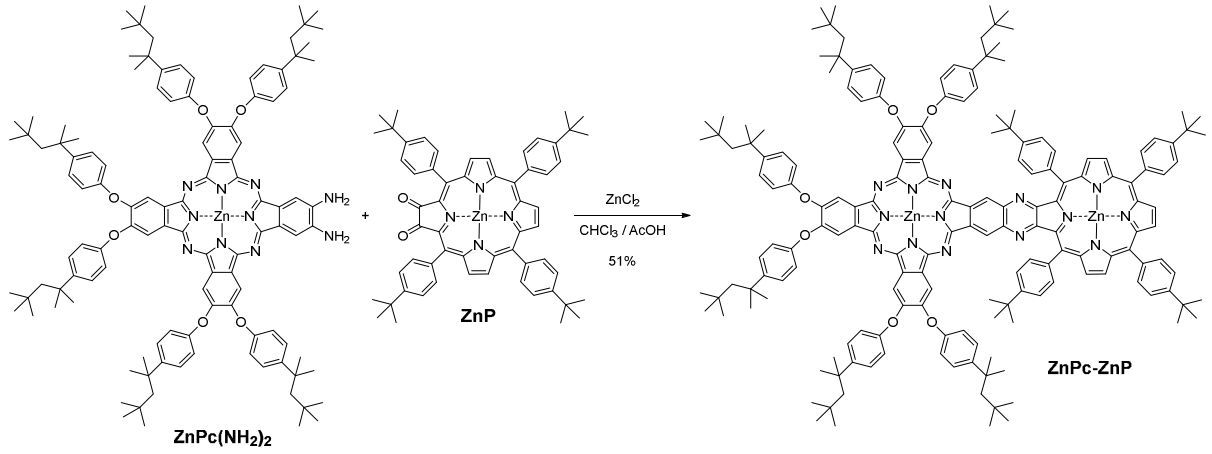

Scheme 1. Synthetic route of ZnPc-ZnP.

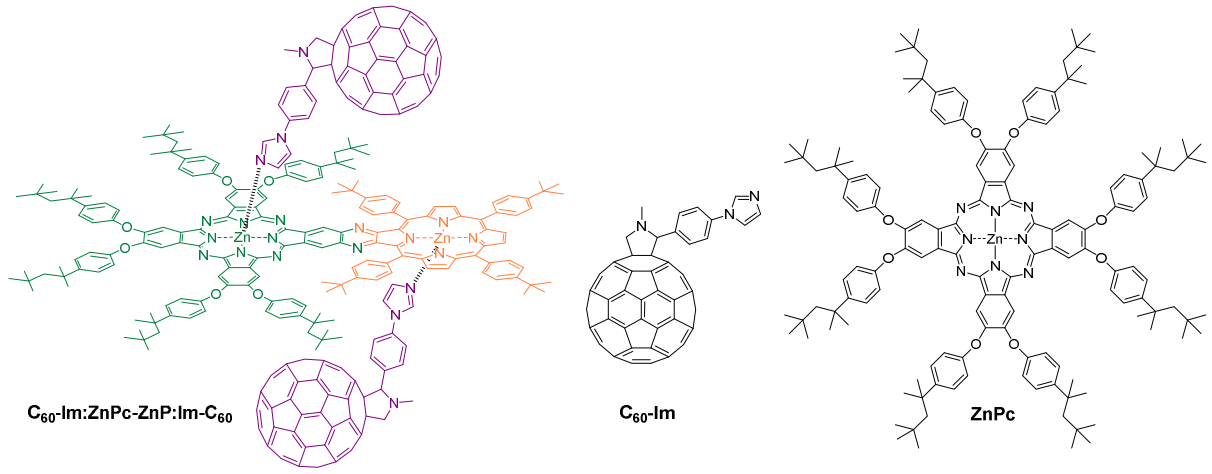

Scheme 2. Molecular structures of C_{60}-Im:ZnPc-ZnP:ImC_{60} supramolecular complex, C_{60}-Im and ZnPc control compound.

View Article Online
DOI: 10.1039/C8CP00382C

Results and Discussion

Synthesis and characterization

The synthesis of ZnPc-ZnP was accomplished by condensation of 1,2-diaminophthalocyanine [$ZnPc(NH_2)_2$] and 2,3-dioxoporphyrin (ZnP) in a mixture of $CHCl_3$/AcOH. During the course of the reaction, $ZnCl_2$ was added to the reaction mixture, yielding a 51% of the ZnPc-ZnP fused dyad (**Error! Reference source not found.**). The *tert*-octylphenoxy groups in the phthalocyanine ring were chosen to avoid π-π staking and, as a consequence, aggregation. The phthalocyanine and porphyrin precursors were prepared as previously described in the literature.[40–42] The synthesized ZnPc-ZnP dyad was fully characterized using ^{1}H-NMR, UV-vis absorption and emission spectroscopies and HR-MALDI-TOF mass spectrometry. Figure 1 shows the ^{1}H-NMR spectrum of ZnPc-ZnP covering the aromatic region in THF-d_8 as solvent. All the signals have been assigned by comparing individual spectra of $ZnPc(NH_2)_2$ and ZnP precursors, and also with the aid of a COSY experiment (see SI). It is worth noting that the de-shielded singlet at 9.88 ppm corresponding to the pyrazine-fused benzene ring demonstrates the conjugation between both subunits. Finally, HR MALDI-TOF MS experiment showed the expected molecular ion peak at m/z= 2726.3835 shows an isotopic distribution that exactly matched the simulated isotopic patterns for $C_{176}H_{192}N_{14}O_6Zn_2$ ([M^+] of the ZnPc-ZnP complex, see SI).

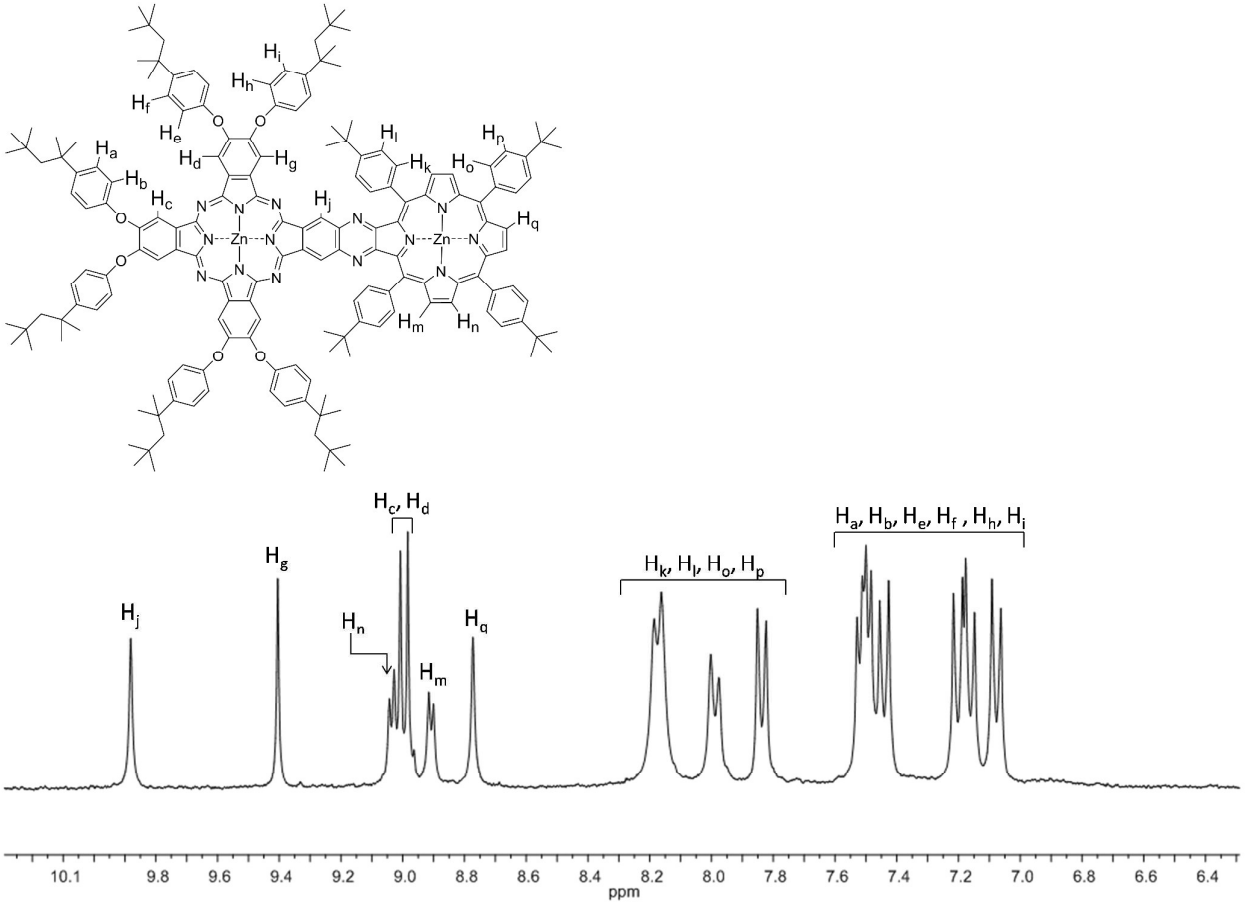

Figure 1. ^{1}H-NMR spectra of ZnPc-ZnP in THF-d_8.

Figure 2a shows the UV-Vis spectra of the highly conjugated ZnPc-ZnP dyad along with those of the reference compounds in toluene (see Figure S1 for structures of control compounds). Absorption peak maxima of ZnP were located at 417, 428 and 492 nm while that of ZnPc were located at 354, 616, and 684 nm. The spectrum recorded for a 1:1 mixture of ZnP and ZnPc was a simple addition of the individual monomers in solution indicating lack of intermolecular interactions between them. Interestingly, the spectrum of ZnPc-ZnP dyad revealed significant changes, peaks at 360, 415, 488 (sh), 645, 682 and 720 nm were observed. The peak corresponding to ZnPc Q band of the ZnPc-ZnP dyad was red

View Article Online
DOI: 10.1039/C8CP00382C

shifted by 36 nm due to fusion of these two rings extending their π-conjugation. Moreover, the split Soret band of ZnP emerged as a single peak in the dyad. These results were indicative of strong electronic coupling between the two π-systems facilitated by the fused linker, however, still retaining basic absorption spectral pattern of ZnPc and ZnP.

The fluorescence spectra recorded for the dyad and the control compounds also revealed interesting results. The emission spectrum of ZnP was broad spanning the 600-725 nm region with a maxima at 610 nm (Figure 2b). The emission maxima for ZnPc was located at 690 nm when excited at the visible peak maxima. The fluorescence spectrum recorded for the 1:1 mixture of ZnP and ZnPc at the excitation wavelength of 417 nm, corresponding to ZnP Soret band, revealed peaks at 610 nm with same intensity to that of pristine ZnP with an additional peak at 690 nm due to direct excitation of ZnPc at this wavelength. The absence of quenching of ZnP emission in the mixture once again confirmed the lack of intermolecular interactions between the two entities. Interestingly, the fluorescence spectrum recorded for the ZnPc-ZnP dyad at the excitation wavelength of 417 nm revealed a total lack of ZnP emission but a strong emission at 742 nm corresponding to ZnPc. In a control experiment, the emission peak at 742 nm due to ZnPc emission was confirmed by direct excitation of ZnPc in the dyad. The redshift is due to extended conjugation effect similar to that observed in the absorption spectrum of the ZnPc-ZnP dyad. These results are indicative of occurrence of very efficient singlet-singlet energy transfer from the ^{1}ZnP* to ZnPc within the dyad.[43] Excitation spectrum recorded for the dyad by holding the emission wavelength to ZnPc emission and scanning the excitation wavelength revealed peaks corresponding to both ZnP and ZnPc entities thus confirming the occurrence of excitation transfer in the dyad (see Figure S16).

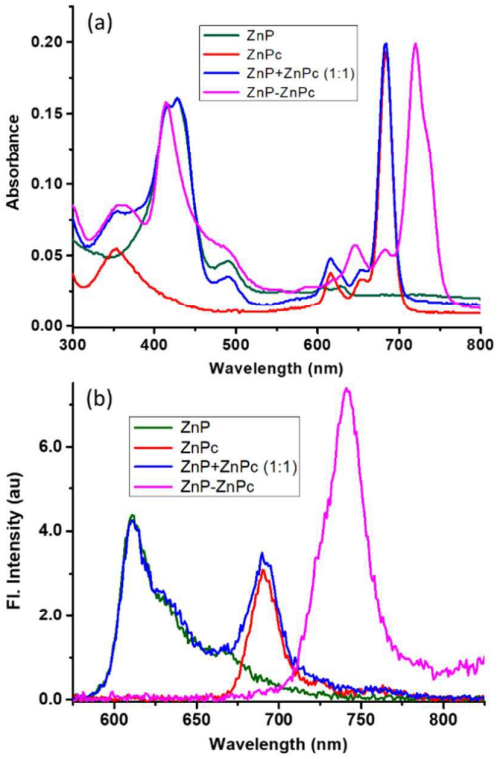

Figure 2. (a) Normalized UV-Vis absorption and (b) fluorescence spectra of ZnPc-ZnP (magenta), ZnPc (red), ZnP (dark green) and 1:1 mixture of ZnP and ZnPc (blue) in toluene (λ_{ex} = 417 nm corresponding to ZnP).

^{1}H NMR studies of supramolecular complexation

In order to quantitatively evaluate the supramolecular interaction between ZnPc-ZnP and C_{60}Im, ^{1}H-NMR studies were performed probing the complexation behavior of C_{60}Im with the dyad, and with control ZnPc and ZnP compounds (see Scheme 1 and Scheme 2 for molecular structures). It may be mentioned here that in the present study, we have utilized three non-coordinating solvents, viz., chloroform (d1) for NMR titrations, toluene for spectral and transient spectral studies due to its higher stability for laser light, and dichlorobenzene for electrochemical measurements since the supporting electrolytes are soluble in this solvent and not in toluene. However, the binding properties (in terms of binding constant and stoichiometry) remain almost same in these solvents.[32]

View Article Online
DOI: 10.1039/C8CP00382C

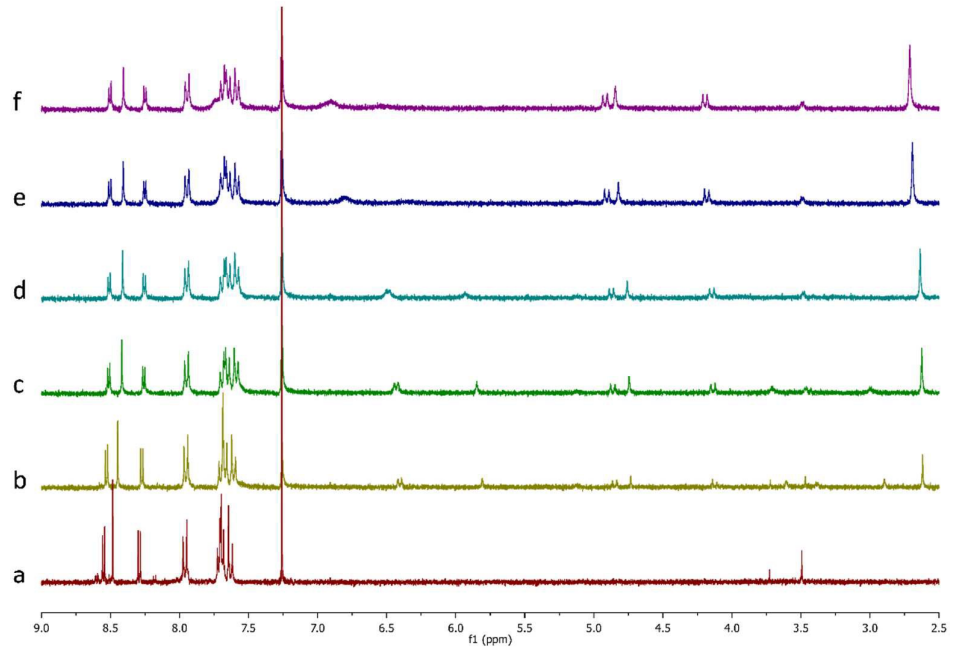

Figure 3. ^{1}H-NMR spectra of a $CDCl_3$ solution of ZnP upon addition of a) 0 equiv, b) 0.44 equiv c) 0.85 equiv d) 1.00 equiv e) 1.54 equiv and f) 1.98 equiv, of C_{60}Im.

Upon addition of increasing amounts of C_{60}Im, while keeping the concentration of ZnP constant in a $CDCl_3$ solution (Figure 3), upfield shifting of all ZnP signals was observed. For example, the doublet centered at 8.55 ppm was shifted to 8.50 ppm, and a similar chemical displacement upon C_{60}Im interaction was observed for rest of the ZnP hydrogens. New signals concomitantly appeared, while increasing their intensity, ascribed to C_{60}Im. As an example, when 0.44 equivalent of C_{60}Im was added, imidazole-hydrogen signals could be distinguished as three singlets centered at 5.81, 3.60 and 2.88 ppm. These signals were gradually down field shifted to 5.83, 3.66 and 2.95 ppm when 1 equivalent of C_{60}Im was added (Figure 3d). Further increased addition caused binding-induced broadening of the signals due to slow chemical exchange under the experimental conditions used. Analysis of such NMR changes clearly suggested a ZnP:ImC_{60} 1:1 stoichiometry, with no need of additional experiments. Finally, global nonlinear least-squares curve-fitting analysis of complexation shift (Δδ) of seven different host (ZnP) signals, afforded a value for the association constant ($K_{C60Im:ZnP}$), of 2.3 x 10^4 M^{-1} (see SI).

Following the same methodology, the interaction between C_{60}Im and ZnPc was studied but, in this case, adding increasing quantities of ZnPc (guest) while keeping the concentraton of C_{60}Im constant (Host). The reason for that is the low resolution of ZnPc NMR spectrum in $CDCl_3$, which makes difficult to acquire reliable data in early titration stages. The analysis of NMR changes clearly suggested again a C_{60}Im:ZnPc 1:1 stoichiometry, while global nonlinear least-squares curve-fitting analysis of complexation shift (Δδ) of five different host (C_{60}Im) signals, afforded a value for the association constant ($K_{C60Im:ZnPc}$), of 1.6 x 10^4 M^{-1} (see SI). And finally, an analogue titration experiment was performed, adding increasing quantities of C60Im to a ZnPc-ZnP $CDCl_3$ solution. This experimental setup was chosen on purpose due to difficulty in acquiring realiable data in the early stages of titration, and also due to the complexity of fitting experimental data to a 2:1 binding profile equations. In this case, seven selected signals were globally analyzed and non-linearly fitted to 1:1 and 1:2 Host/Guest systems, and found that 1:2 fitting was more accurate than 1:1, expected due to ZnPc-ZnP molecular structure (see SI). These results are indicative of a supramolecular C_{60}Im:ZnPc-ZnP:ImC_{60} complex formation. According to Thordarson *et col*,[44] intermolecular cooperativity is present in a 1:2 complex of a divalent host and two monovalent guests if $K_1 \neq K_2$, but in a non-cooperative case, "the two intrinsic binding constants are equal and (ideally) identical to that of a monovalent reference complex". This seems to be our case because the obtained values for K_1 and K_2, 0.8 x 10^4 and 2.4 x 10^4 M^{-1} respectively, are close to those obtained for individual control compounds suggesting lack of cooperative binding effect. One could also imagine the supramolecular complex to assume a *trans* 1:2 structure with the two fullerenes on the opposite sides of the dyad or a *syn* structure having both fullerenes at the same side of the dyad. Computational studies were performed to visualize such structures and their energies (*vide infra*).

UV-visible Spectral and Computational Studies of the Supramolecular Donor-Acceptor Complex Formation

Figure 4a shows the UV-Vis spectral changes observed for ZnPc-ZnP dyad upon increasing addition of C_{60}Im in toluene

View Article Online
DOI: 10.1039/C8CP00382C

which also point out to the formation of the supramolecular C_{60}Im:ZnPc-ZnP:ImC_{60} complex.[33,34] Peaks located at 645 and 720 nm revealed a decrease in intensity with the appearance of isosbestic points at 658, 692 and 755 nm. The binding constants were evaluated by analyzing the spectral data according to the Benesi-Hildebrand method.[45] Such analysis yielded K_1 and K_2 values of 5.4 x 10^4 M^{-1} and 6.8 x 10^4 M^{-1}, respectively. The magnitude of these values is comparable to earlier discussed binding constants obtained from NMR

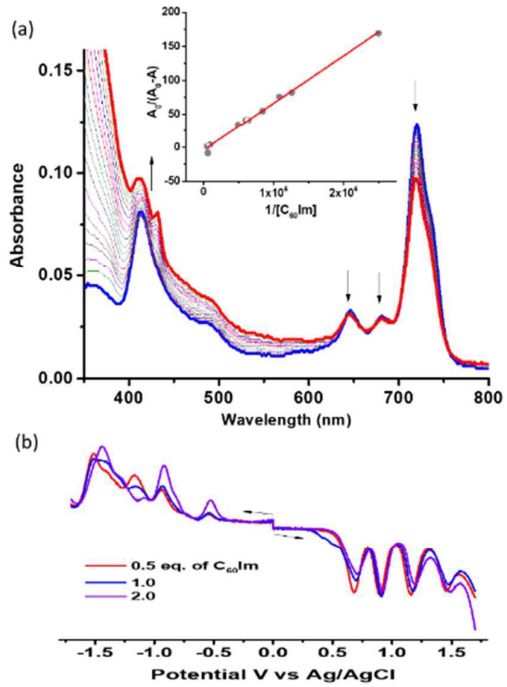

Figure 4. (a) Spectral changes observed after addition of increasing amounts of C_{60}Im to a 2 μM solution of ZnPc-ZnP in toluene. (b) Differential pulse voltammograms during the course of supramolecular C_{60}Im:ZnPc-ZnP:ImC_{60} complex formation (0.05 mM ZnPc-ZnP and up to 2 equivalents of C_{60}Im) in dichlorobenzene containing 0.1 M $TBAClO_4$

titrations. And also slightly smaller to those previously obtained by UV-vis titrations of *o*-dichlorobenzene ZnP and ZnPc solutions with C_{60}Im (2.1 x 10^4 M^{-1} and 1.3 x 10^5 M^{-1}, respectively.[46,47] This fact can be attributed to experimental error caused by overlapping absorption peaks of bound and unbound species at the monitoring wavelength. The mole ratio plot also revealed 1:1 binding to each metal site within the dyad.

As shown in Figure S13, fluorescence spectrum of the ZnPc-ZnP dyad revealed quenching of the 742 nm band corresponding to ^{1}ZnPc* upon increasing addition of C_{60}Im, when either directly excited at 720 nm corresponding to ZnPc or excited at 420 nm corresponding to the Soret peak of ZnP. The calculated fluorescence quantum yield (Φ_f) for the dimer was found to be 0.06 (reference ZnPc, Φ_f = 0.07[48]) that was reduced to about 35% of the original value upon coordinating the fullerene. These results suggest additional photochemical events from ^{1}ZnPc* formed either by direct excitation or by excitation transfer from ^{1}ZnP* in the supramolecular C_{60}Im:ZnPc-ZnP:ImC_{60} complex.

Figure 4b shows the differential pulse voltammograms during the course of C_{60}Im:ZnPc-ZnP:ImC_{60} complex formation. The first three oxidations and reductions of ZnPc-ZnP were located at 0.67, 0.88, 1.34, -0.95, -1.37 and -1.48 V vs. Ag/AgCl. Cyclic voltammetry experiments confirmed that these processes were reversible to quasireversible (see Figure S14 in SI). By comparing the voltammograms of control ZnP and ZnPc compounds, the first oxidation process to ZnPc and the second one to ZnPc within the dyad was possible to arrive. As shown in Figure 4b, successive addition of C_{60}Im to the solution of ZnPc-ZnP revealed notable changes. That is, anodic shift of about 40 mV of the first oxidation due to ZnPc:ImC_{60} formation, and about 20 mV shift of the second oxidation due to ZnP-ImC_{60} formation, were noted. The first reduction of the C_{60}Im:ZnPc-ZnP:ImC_{60} complex was located at -0.53 V *vs.* Ag/AgCl corresponding to $C_{60}^{0/-\cdot}$ formation. Additional reductions of C_{60} at more negative potentials, often overlapping with the reductions of other entities within the complex were observed. These results provide evidence of metal-ligand axial coordination induced subtle redox changes in the supramolecular complex.

The structure of the ZnPc-ZnP dyad and the supramolecular C_{60}Im:ZnPc-ZnP:ImC_{60} complex were optimized at the B3LYP/6-31G(dp) for H, C, and N, and 6-31G(df) for Zn level on *Gaussian 09*.[49] The structures were fully optimized on a Born-Oppenheimer potential energy surface. Figure S15 shows the optimized structure of ZnPc-ZnP on the edge-on and side-on orientations (i and ii). As predicted for the fused dyad, an almost perfect coplanar structure was obtained (dihedral angle < 1°). The Zn-Zn distance between the two metal centers was found to be 13.3 Å revealing close proximity. The frontier orbitals, HOMO and LUMO, were found to be delocalized over both the rings in agreement with the earlier discussed strong electronic coupling between the two π-systems. Further, to visualize the geometry of the supramolecular structures, two structures one in which the two C_{60}Im units occupy the opposite faces of the dyad, *trans*-isomer and the second one in which both C_{60}Im occupy the same side of the ZnPc-ZnP dyad, *syn*-isomer (see Figure 5 i and ii). Energy calculations revealed that the *trans*-isomer is moderatively favorable by 0.088 kcal. This could be largely attributed to less steric hindrance in the *trans* structure. In the optimized structure, the HOMO was delocalized over the entire dyad π -system, while the LUMO was found to be localized over the C_{60} entity (Figure 5, iii), establishing the donor and acceptor identity within the supramolecular system. Such delocalization of the HOMO is known to stabilize the charge separated state.[50,51]

View Article Online
DOI: 10.1039/C8CP00382C

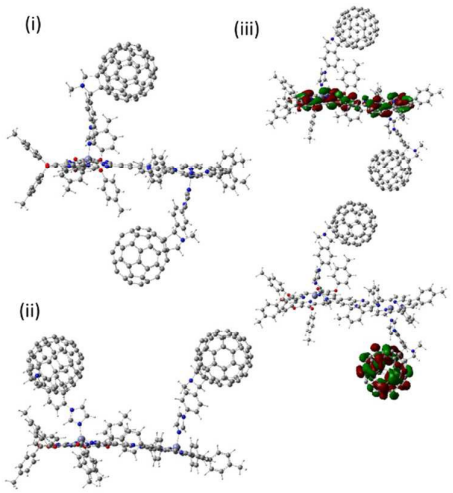

coordinated fullerene was thermodynamically possible in the supramolecular C_{60}Im:ZnPc-ZnP:ImC_{60} complex. However, as discussed earlier, excitation of ZnP in the triad could also promote energy transfer efficiently.

Figure 5. B3LYP/6-31G(dp) optimized structure of C_{60}Im:ZnPc-ZnP:ImC_{60} (i) in the *trans* and (ii) *syn* configurations and (iii) frontier HOMO and LUMO of the *trans* structure.

Transient Absorption Studies to Probe Charge Separation

Femtosecond transient absorption spectral studies of the ZnPc-ZnP dyad along with the control compounds were performed in toluene. The fluorescence studies had revealed an almost complete quenching of ZnP fluorescence accompanied by the appearance of the ZnPc emission indicating a very efficient singlet-singlet energy transfer in the dyad. Figure 6a shows the transient spectra of ZnPc-ZnP at the excitation wavelength of 417 nm (100 fs pulses) where ZnP is mainly excited. The transient spectra for the ZnP and ZnPc are shown in SI (Figure S11). The transient signals of ZnP were

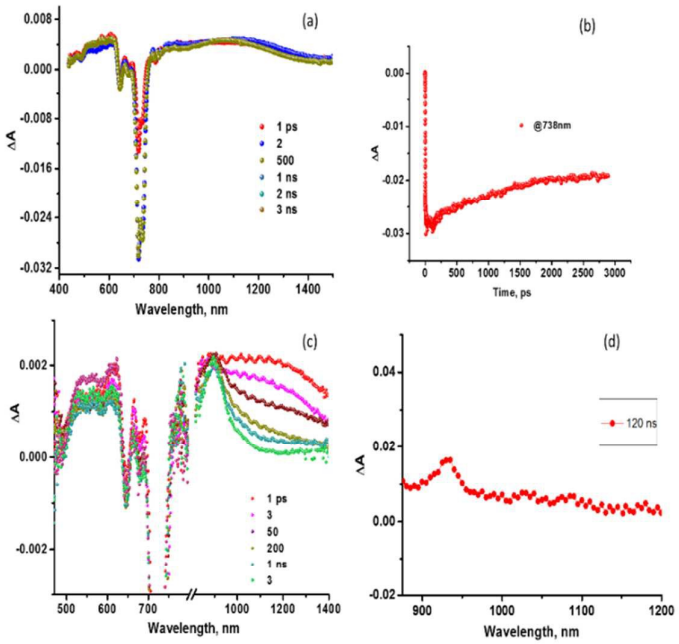

Figure 6. (a) Femtosecond transient absorption spectra of ZnPc-ZnP (0.05 mM in a 2 mm path length cell) in toluene at the excitation wavelength of 417 nm. (b) Time profile of the 738 nm peak corresponding to ZnP stimulated emission. (c and d) Femto- and nanosecond transient spectra of supramolecular C_{60}Im:ZnPc-ZnP:ImC_{60} complex (0.05 mM) in toluene at 417 nm excitation.

From the spectral, computational and redox data, free-energy changes for light induced energy and/or electron transfer within ZnPc-ZnP dyad and of the C_{60}Im:ZnPc-ZnP:ImC_{60} supramolecular complex were evaluated using the Rehm and Weller approach.[52,§] Such calculations revealed that energy transfer from ^{1}ZnP* to ZnPc in the dyad and supramolecular traid are both feasible by ~0.3 eV. Additionally, charge separation in the C_{60}Im:ZnPc-ZnP:ImC_{60} supramolecular complex from the ^{1}ZnP* was exothermic by -0.57 eV, while from the ^{1}ZnPc* it was -0.46 eV. That is, charge separation from either of the singlet excited states of donors to the located at 473, 594, 657, 1050 and 1192 nm corresponding to transitions originating from the singlet excited state (see Figure S11a-b). In addition, negative peaks at 580 nm corresponding to ground state bleaching and at 630 and 698 nm corresponding to stimulated emission were also observed. Time decay/recovery of these signals resulted in new spectral features corresponding to ^{3}ZnP* with peaks at 483 and 858 nm. The transient spectra of ZnPc revealed positive peaks at 443, 504, 545, 740 and 1160 nm due to singlet excited state originated transitions, and a negative peak at 615 nm due to ground state bleaching and another at 684 due to stimulated emission (Figure S11c-d).

View Article Online
DOI: 10.1039/C8CP00382C

Interestingly, the spectra of the ZnPc-ZnP dyad shown in Figure 6a revealed only peaks corresponding to ^{1}ZnPc* although the dyad was excited at a wavelength where ZnP absorbs predominantly. These results indicate the occurrence of ultrafast energy transfer in less than 1.9 ps (close to the time resolution of transient setup) from ^{1}ZnP* to ZnPc leading to the formation of ^{1}ZnPc* within the dyad. The time profile of the ZnPc peak in the dyad (Figure 6b) tracked closely to that of control ZnPc in Figure S11d suggesting the lack of further photochemical reactions from ^{1}ZnPc* to ZnP within the dyad. The estimated singlet-singlet energy transfer rate constant was $k_{EnT} > 10^{12}$ s^{-1} for the dyad.

Next, photoinduced electron transfer in the supramolecular C_{60}Im:ZnPc-ZnP:ImC_{60} complex was investigated. The rate constants for electron transfer in the control dyads were reported to be k_{ET} = 5.7 x 10^9 s^{-1} for the C_{60}Im:ZnPc dyad[46] and k_{ET} = 5.0 x 10^9 s^{-1} for the ZnP:ImC_{60} dyad.[47] These rate constants are about 3 orders of magnitude

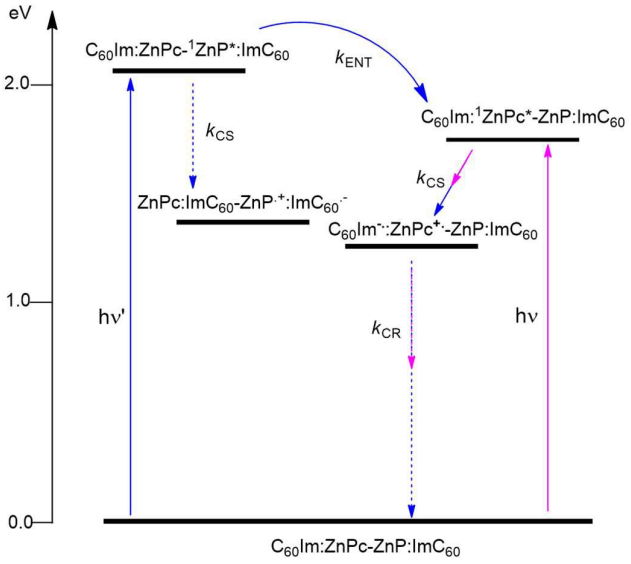

Scheme 3. Photochemical events occurring in the supramolecular C_{60}Im:ZnPc-ZnP:ImC_{60} complex upon excitation of ZnP (blue arrows) and ZnPc (magenta arrows). Solid lines represent major photochemical events while the dashed line show minor photochemical event. (ENT = energy transfer, CS = charge separation, CR = charge recombination).

smaller than the earlier discussed k_{EnT} value in the dyad. Under these conditions, excitation of ZnP in the C_{60}Im:ZnPc-ZnP:ImC_{60} complex would preferentially promote energy transfer to ZnPc over electron transfer to the coordinated C_{60}Im. Conversely, the ^{1}ZnPc* which is formed via energy transfer process or by direct excitation can undergo electron transfer to the coordinated C_{60}Im yielding the ZnPc$^{\bullet+}$:Im$C_{60}^{\bullet-}$ charge separated state. Thus, it can be anticipated that in the novel supramolecular complex one photon promoting two photochemical events (sequential energy and electron transfer processes) as shown in the energy level diagram in Scheme 3 (photochemical path shown in blue arrows).

This is indeed to be the case as shown by the transient spectral data in Figure 6c. Immediately after excitation of ZnP, formation of ^{1}ZnPc* was obvious (see spectrum at 1 ps) revealing ultrafast energy transfer. Similar to the ZnP-ZnPc dyad, no peaks originating from the ^{1}ZnP* could be observed. The decay/recovery of the ^{1}ZnPc* peaks was accompanied by new peaks at 900 and 1020 nm (shoulder band) corresponding to ZnPc$^{\bullet+}$ (Figure S12) and Im$C_{60}^{\bullet-}$ species providing evidence for the occurrence of electron transfer in the supramolecular complex. By monitoring the time profiles, the determined rate constant for charge separation, k_{CS} was found to be 4.35 x 10^9 s^{-1}. The quantum yield for charge separation, (Φ_{cs})[53] was found to be about 10.6%. As shown in the spectrum recorded at 3 ns (maximum delay time of our instrument setup), the radical ion-pair peaks were still present. This is in agreement with the earlier discussed delocalization of the HOMO over the entire dyad expecting to slow down the charge recombination process. Further, nanosecond transient spectral measurements were performed to exactly determine the lifetime of the charge separated state. As shown in Figure 6d, the spectrum recorded at 120 ns had signature peaks of both ZnPc$^{\bullet+}$ and Im$C_{60}^{\bullet-}$ species thus confirming charge stabilization in the supramolecular complex. A complete disappearance of the radical ion spectrum was observed around at 200 ns.

Conclusions

In summary, the ZnPc-ZnP dyad fused through a pyrazine ring revealed strong electronic interactions between the two entities, and revealed an optimized geometry in which the two macrocycle rings were in the same plane. The good spectral overlap between the emission of ZnP and absorption of ZnPc along with planar geometry with highly delocalized HOMO and LUMO promoted efficient singlet-singlet energy transfer with an estimated rate of $k_{EnT} > 10^{12}$ s^{-1}. The ZnPc-ZnP dyad acted as a host to accommodate two C_{60}Im entities via metal-ligand axial coordination in which the resulting geometry of the supramolecular C_{60}Im:ZnPc-ZnP:ImC_{60} complex had two geometric possibilities, viz., *trans*- and *syn*-isomers. The possibility of occurrence of photoinduced electron transfer in the supramolecular complex was arrived from free-energy calculations performed using spectral, electrochemical and computational data. Transient absorption studies performed using the wide femto- to millisecond time scale conclusively provided evidence of charge separation in which the charge separated state was ZnPc$^{\bullet+}$:Im$C_{60}^{\bullet-}$-ZnP:ImC_{60}. Owing to the delocalization of ZnPc$^{\bullet+}$ over the entire π-system, the charge separated state was found to be long-lived that persisted for about 200 ns prior returning to the ground state.

Experimental Section

Synthesis

All solvents were used as received from Sigma-Aldrich. ^{1}H NMR spectra were recorded at 25°C using a Bruker AC300 spectrometer, and were referenced to tetramethylsilane. The solvent for spectroscopic studies was of spectroscopic grade and used as received. The UV-visible spectral measurements

View Article Online
DOI: 10.1039/C8CP00382C

were carried out with either a Helios Gamma or Shimadzu Model 2550 double monochromator UV-visible spectrophotometer. The fluorescence emission was monitored by using a Varian Eclipse spectrometer. A right angle detection method was used. High-resolution mass spectra were obtained from a Bruker Microflex LRF20 matrix-assisted laser desorption/ionization time-of-flight (MALDI-TOF) using dithranol as matrix. Differential pulse voltammograms were recorded on an EG&G 263A potentiostat/galvanostat using a three electrode system: a platinum button electrode was used as the working electrode, a platinum wire served as the counter electrode and an Ag/AgCl electrode was used as the reference electrode. Ferrocene/ferrocenium redox couple was used as an internal standard. Tetra-*n*-butylammonium perchlorate, (n-Bu_4N)ClO_4, used in electrochemical studies was from Fluka Chemical. All the solutions were purged prior to electrochemical and spectral measurements using nitrogen gas. Buckminsterfullerene C_{60} (+99.95%) was from SES Research (Houston, TX). Synthesis of C_{60}Im is described elsewhere.[54]

ZnPc-ZnP: A mixture of $ZnPcNH_2$ (39 mg, 0.02 mmol),[40] ZnP (9 mg, 0.01 mmol),[41,42] acetic acid (2 drops), $ZnCl_2$ (2.9 mg, 0.02 mmol) in $CHCl_3$ (0.2 mL) was heated to reflux under argon overnight. Then, the crude was diluted with $CHCl_3$ and washed with H_2O. The organic layer was dried with $MgSO_4$, concentrated in vacuum and purified by column chromatography (DCM/AcOEt), affording 14 mg (51%) of ZnPc-ZnP. ^{1}H NMR (300 MHz, THF-d_8, 25ºC): δ = 9.88 (s, 2H), 9.40 (s, 2H), 9.04 (d, 2H), 9.01 (s, 2H), 8.98 (s, 2H), 8.91 (d, 2H), 8.77 (s, 2H), 8.18 (d, 8H), 8.00 (d, 4H), 7.85 (d, 4H), 7.53-7.43 (m, 12H), 7.22-7.06 (m, 12H), 1.98 (s, 12H), 1.64 (s, 36H), 1.49-1.42 (m, 36H), 0.87-0.83 (m, 54H). UV-vis ($CHCl_3$): λ_{max}/nm (log Ɛ): 358 (4.82), 415 (5.06), 644 (4.59), 716 (5.18). HRMS (MALDI-TOF): m/z for $C_{176}H_{192}N_{14}O_6Zn_2$ calcd, 2726.3805; found, 2726.3835.

Femtosecond Pump-Probe Transient Spectroscopy

Femtosecond transient absorption spectroscopy experiments were performed using an Ultrafast Femtosecond Laser Source (Libra) by Coherent incorporating diode-pumped, mode locked Ti:Sapphire laser (Vitesse) and diode-pumped intra cavity doubled Nd:YLF laser (Evolution) to generate a compressed laser output of 1.45 W. For optical detection, a Helios transient absorption spectrometer coupled with femtosecond harmonics generator both provided by Ultrafast Systems LLC was used. The source for the pump and probe pulses were derived from the fundamental output of Libra (Compressed output 1.45 W, pulse width 100 fs) at a repetition rate of 1 kHz. 95% of the fundamental output of the laser was introduced into a TOPAS-Prime-OPA system with 290-2600 nm tuning range from Altos Photonics Inc., (Bozeman, MT), while the rest of the output was used for generation of white light continuum. In the present study, the second harmonic 400 nm excitation pump was used in all the experiments. Kinetic traces at appropriate wavelengths were assembled from the time-resolved spectral data. Data analysis was performed using Surface Xplorer software supplied by Ultrafast Systems. All measurements were conducted in degassed solutions at 298 K.

Nanosecond Laser Flash Photolysis

The studied compounds were excited by a Opolette HE 355 LD pumped by a high energy Nd:YAG laser with second and third harmonics OPO (tuning range 410-2200 nm, pulse repetition rate 20 Hz, pulse length 7 ns) with the powers of 1.0 to 3 mJ *per* pulse. The transient absorption measurements were performed using a Proteus UV-Vis-NIR flash photolysis spectrometer (Ultrafast Systems, Sarasota, FL) with a fibre optic delivered white probe light and either a fast rise Si photodiode detector covering the 200-1000 nm range or a InGaAs photodiode detector covering 900-1600 nm range. The output from the photodiodes and a photomultiplier tube was recorded with a digitizing Tektronix oscilloscope.

Conflicts of interest

There are no conflicts to declare.

Acknowledgments

Support from the Ministerio de Economía Industria y Competitividad of Spain (CTQ2014-55798-R and CTQ2017-87102-R), the Special Research Account of the University of Crete, and US-National Science Foundation (grant no. 1401188 to FD) is gratefully acknowledged

Notes and references

§ Free-energy calculation for charge-separation (ΔG_{CS}) was performed according to the following equation,

$$-\Delta G_{CS} = \Delta E_{00} - (E_{ox} - E_{red} + \Delta G_S)$$

where ΔE_{00} and ΔG_S correspond to the energy of 0-0 transition of ^{1}ZnP* and ^{1}ZnPc*, and electrostatic energy, respectively. The E_{ox} and E_{red} represent the oxidation potential of the electron donor (ZnPc or ZnP) and the reduction potential of the electron acceptor (C_{60}), respectively. ΔG_S refers to the static energy, calculated by using the 'Dielectric continuum model' according to the following equation,

$$\Delta G_S = e^2/(4\pi\varepsilon_0)[(1/2R_{+} + 1/2R_{\cdot} - 1/R_{CC})(1/\varepsilon_S) - (1/2R_{+} + 1/2R_{\cdot})(1/\varepsilon_R)]$$

where R_+ and $R_\cdot$ are the radio of the radical cation and radical anion, respectively; R_{CC} is the centre-to-centre distances between donor and C_{60}, which were evaluated from the optimized structure. The symbols ε_R and ε_S refer to solvent dielectric constants for electrochemistry and photophysical measurements, respectively.

1 G. Bottari, O. Trukhina, M. Ince and T. Torres, *Coord. Chem. Rev.*, 2012, **256**, 2453–2477.
2 K. V. Rao, K. K. R. Datta, M. Eswaramoorthy and S. J. George, *Chem. – A Eur. J.*, 2012, **18**, 2184–2194.
3 D. F. Perepichka and F. Rosei, *Science (80-.).*, 2009, **323**, 216–217.
4 J. M. Mativetsky, M. Kastler, R. C. Savage, D. Gentilini, M. Palma, W. Pisula, K. Müllen and P. Samorì, *Adv. Funct. Mater.*, 2009, **19**, 2486–2494.
5 S. Günes, H. Neugebauer and N. S. Sariciftci, *Chem. Rev.*, 2007, **107**, 1324–1338.
6 M. Emmelius, G. Pawlowski and H. W. Vollmann, *Angew. Chemie Int. Ed. English*, 1989, **28**, 1445–1471.

View Article Online
DOI: 10.1039/C8CP00382C

7 I. Obraztsov, W. Kutner and F. D'Souza, *Sol. RRL*, 2017, **1**, 1600002.
8 G. Bottari, G. de la Torre, D. M. Guldi and T. Torres, *Chem. Rev.*, 2010, **110**, 6768–6816.
9 Y. Kobuke, *Eur. J. Inorg. Chem.*, 2006, 2333–2351.
10 V. Balzani, A. Credi and M. Venturi, *ChemSusChem*, 2008, **1**, 26–58.
11 S. Fukuzumi and K. Ohkubo, *J. Mater. Chem.*, 2012, **22**, 4575.
12 H. Imahori, T. Umeyama and S. Ito, *Acc. Chem. Res.*, 2009, **42**, 1809–1818.
13 M. R. Wasielewski, *Acc. Chem. Res.*, 2009, **42**, 1910–1921.
14 D. Gust, T. A. Moore and A. L. Moore, *Acc. Chem. Res.*, 2009, **42**, 1890–1898.
15 F. D'Souza and O. Ito, *Multiporphyrin Arrays: Fundamentals and Applications*, Pan Stanford Publishing: Singapore, 2012.
16 C. C. Leznoff and A. B. P. Lever, *Phthalocyanines: Properties and Applications*, WILEY-VCH Verlag, Weinheim, Germany, 1989.
17 N. B. McKeown, *Phthalocyanine Materials: Synthesis, Structure, and Function*, Cambridge University Press, 1998.
18 V. N. Nemykin, S. V. Dudkin, F. Dumoulin, C. Hirel, A. G. Gürek and V. Ahsen, *ARKIVOC*, 2014, 142–204.
19 G. de la Torre, C. G. Claessens and T. Torres, *Chem. Commun.*, 2007, 2000–2015.
20 J. Mack and N. Kobayashi, *Chem. Rev.*, 2011, **111**, 281–321.
21 J.-H. Chou, H. S. Nalwa, M. E. Kosal, N. A. Rakow and K. S. Suslick, *The Porphyrin Handbook*, World Scientific Press, San Diego, 2000.
22 Y. Rio, M. Salome Rodriguez-Morgade and T. Torres, *Org. Biomol. Chem.*, 2008, **6**, 1877–1894.
23 M. V. Martinez-Diaz, G. de la Torre and T. Torres, *Chem. Commun.*, 2010, **46**, 7090–7108.
24 T. Bessho, S. M. Zakeeruddin, C.-Y. Yeh, E. W.-G. Diau and M. Grätzel, *Angew. Chemie Int. Ed.*, 2010, **49**, 6646–6649.
25 J. Malig, N. Jux, D. Kiessling, J.-J. Cid, P. Vázquez, T. Torres and D. M. Guldi, *Angew. Chemie Int. Ed.*, 2011, **50**, 3561–3565.
26 S. Mori, M. Nagata, Y. Nakahata, K. Yasuta, R. Goto, M. Kimura and M. Taya, *J. Am. Chem. Soc.*, 2010, **132**, 4054–4055.
27 J.-J. Cid, M. García-Iglesias, J.-H. Yum, A. Forneli, J. Albero, E. Martínez-Ferrero, P. Vázquez, M. Grätzel, M. K. Nazeeruddin, E. Palomares and T. Torres, *Chem. Eur. J.*, 2009, **15**, 5130–5137.
28 C. B. KC, K. Stranius, P. D'Souza, N. K. Subbaiyan, H. Lemmetyinen, N. V Tkachenko and F. D'Souza, *J. Phys. Chem. C*, 2013, **117**, 763–773.
29 V. Bandi, M. E. El-Khouly, V. N. Nesterov, P. A. Karr, S. Fukuzumi and F. D'Souza, *J. Phys. Chem. C*, 2013, **117**, 5638–5649.
30 G. de la Torre, G. Bottari, M. Sekita, A. Hausmann, D. M. Guldi and T. Torres, *Chem. Soc. Rev.*, 2013, **42**, 8049–8105.
31 M. E. El-Khouly, O. Ito, P. M. Smith and F. D'Souza, *J. Photochem. Photobiol. C Photochem. Rev.*, 2004, **5**, 79–104.
32 C. B. KC and F. D'Souza, *Coord. Chem. Rev.*, 2016, **322**, 104–141.
33 A. M. V. M. Pereira, A. Hausmann, J. P. C. Tomé, O. Trukhina, M. Urbani, M. G. P. M. S. Neves, J. A. S. Cavaleiro, D. M. Guldi and T. Torres, *Chem. - A Eur. J.*, 2012, **18**, 3210–3219.
34 C. B. KC, K. Ohkubo, P. A. Karr, S. Fukuzumi and F. D'Souza, *Chem. Commun.*, 2013, **49**, 7614–7616.
35 R. F. Enes, J.-J. Cid, A. Hausmann, O. Trukhina, A. Gouloumis, P. Vázquez, J. A. S. Cavaleiro, A. C. Tomé, D. M. Guldi and T. Torres, *Chem. - A Eur. J.*, 2012, **18**, 1727–1736.
36 C. B. KC, G. N. Lim and F. D'Souza, *Nanoscale*, 2015, **7**, 6813–6826.
37 A. M. V. M. Pereira, A. R. M. Soares, A. Hausmann, M. G. P. M. S. Neves, A. C. Tome, A. M. S. Silva, J. A. S. Cavaleiro, D. M. Guldi and T. Torres, *Phys. Chem. Chem. Phys.*, 2011, **13**, 11858–11863.
38 H. Sato, K. Tashiro, H. Shinmori, A. Osuka, Y. Murata, K. Komatsu and T. Aida, *J. Am. Chem. Soc.*, 2005, **127**, 13086–13087.
39 L. Moreira, J. Calbo, J. Aragó, B. M. Illescas, I. Nierengarten, B. Delavaux-Nicot, E. Ortí, N. Martín and J.-F. Nierengarten, *J. Am. Chem. Soc.*, 2016, **138**, 15359–15367.
40 V. M. Blas-Ferrando, J. Ortiz, K. Ohkubo, S. Fukuzumi, F. Fernández-Lázaro and Á. Sastre-Santos, *Chem. Sci.*, 2014, **5**, 4785–4793.
41 P. Thordarson, A. Marquis and M. J. Crossley, *Org. Biomol. Chem.*, 2003, **1**, 1216–1225.
42 S. Shi, X. Wang, Y. Sun, S. Chen, X. Li, Y. Li and H. Wang, *J. Mater. Chem.*, 2012, **22**, 11006–11008.
43 J. R. Lakowicz, *Principles of Fluorescence Spectroscopy*, Springer, Singapore, 3rd ed., 2006.
44 L. K. S. von Krbek, C. A. Schalley and P. Thordarson, *Chem. Soc. Rev.*, 2017, **46**, 2622–2637.
45 H. A. Benesi and J. H. Hildebrand, *J. Am. Chem. Soc.*, 1949, **71**, 2703–2707.
46 S. K. Das, B. Song, A. Mahler, V. N. Nesterov, A. K. Wilson, O. Ito and F. D'Souza, *J. Phys. Chem. C*, 2014, **118**, 3994–4006.
47 S. K. Das, A. Mahler, A. K. Wilson and F. D'Souza, *ChemPhysChem*, 2014, **15**, 2462–2472.
48. A. Ogunsipe, D. Maree, T. Nyokong, *J. Molecular Structure*, 2003, **60**, 131-140
49 Gaussian09, *Revission B.01*, Gaussian Inc., Pittsburg PA, 2009.
50 F. D'Souza, S. Gadde, D.-M. S. Islam, C. A. Wijesinghe, A. L. Schumacher, M. E. Zandler, Y. Araki and O. Ito, *J. Phys. Chem. A*, 2007, **111**, 8552–8560.
51 C. A. Wijesinghe, M. E. El-Khouly, M. E. Zandler, S. Fukuzumi and F. D'Souza, *Chem. - A Eur. J.*, 2013, **19**, 9629–9638.
52 D. Rehm and A. Weller, *Isr. J. Chem.*, 1970, **8**, 259–271.
53. R. Chitta, A. S. D. Sandanayaka, A. L. Schumacher, L. D'Souza, Y. Araki, O. Ito, F. D'Souza, *J. Phys. Chem. C* 2007, **111**, 6947-6955.
54 F. D'Souza, G. R. Deviprasad, M. E. Zandler, V. T. Hoang, A. Klykov, M. VanStipdonk, A. Perera, M. E. El-Khouly, M.

View Article Online
DOI: 10.1039/C8CP00382C

Fujitsuka and O. Ito, *J. Phys. Chem. A*, 2002, **106**, 3243–3252.

View Article Online
DOI: 10.1039/C8CP00382C

Table of Contents

FULL PAPER

A zinc porphyrin-zinc phthalocyanine, fused at the macrocycle periphery is shown to undergo ultrafast energy transfer followed by electron transfer to coordinated fullerene resulting into long-lived charge separation.

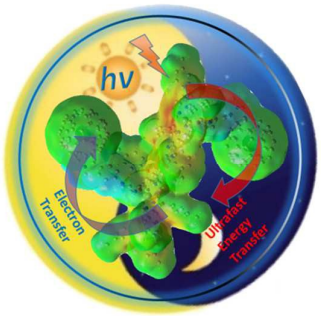

J. Follana-Berná, S. Seetharaman, L. Martín-Gomis, G. Charalambidis, A. Trapali, P. A. Karr, A. G. Coutsolelos, F. Fernández-Lázaro, F. D'Souza and Á. Sastre-Santos**

Page No. – Page No.

Supramolecular Complex of a Fused Zinc Phthalocyanine-Zinc Porphyrin Dyad Assembled by Two Imidazole-C_{60} Units: Ultrafast Energy Transfer Followed by Electron Transfer